Preprints of the 21st IFAC World Congress (Virtual)
Berlin, Germany, July 12-17, 2020

Optimal Frequency Restoration of Inverter-Interfaced Microgrids via Distributed Energy Management

Yiqiao Xu * **Alessandra Parisio** * **Zhengtao Ding** *

* *Department of Electrical and Electronic Engineering, University of Manchester, Manchester, UK (e-mail: yiqiao.xu@postgrad.manchester.ac.uk; alessandra.parisio@manchester.ac.uk; zhengtao.ding@manchester.ac.uk)*

Abstract: Despite the potential role of microgrids is well recognized in supporting the integration of renewable energy sources into the future power system, the impacts of intermittence renewable generation on the microgrid frequency stability is still being explored, and the related challenges remain to be addressed. In this paper, we focus on an islanded inverter-interfaced microgrid and present a consensus-based gradient algorithm for optimal frequency restoration via distributed energy management, preserving the standard hierarchical control architecture but merging the interdependent layers. The network-preserving model is applied to prevent loss of network topology and transient characteristics. Furthermore, not only distributed generators but also demand-side customers are considered to be actively participating in the proposed architecture. Convergence analysis implies that the closed-loop system is asymptotically stable, and its equilibrium will converge to the optimal solution of the associated energy management problem, which is consistent with the observation from the simulation study, including intermittent generation and load perturbation, carried out on a 6-bus test microgrid system. Therefore, the effectiveness of the proposed algorithm is verified.

Keywords: Distributed Optimization, Microgrid, Frequency Restoration, Energy Management.

1. INTRODUCTION

Over recent decades extensive attention has been paid to the role of microgrids to accelerate the integration of renewable energy sources into the traditional electrical grid. A microgrid is generally classified as a small-scale power system composed of multiple distributed generation (DG) units, energy storage devices, and loads at the distribution level, which can operate either in grid-connected or islanded mode. A stable operating point is essential to the normal operation of an islanded microgrid; hence, the so-called grid-forming units are necessitated to provide a synchronous frequency and a certain voltage level at all buses. We refer the readers to Lasseter and Paigi (2004); Dimeas and Hatziargyriou (2005); Katiraei and Iravani (2006) for further details. Therefore, the coordination of all grid-forming units is crucial to the operation of microgrids, but it remains an open challenge due to the intermittent nature of renewable sources, especially at high penetration levels.

Although the coordination and control strategies of a microgrid may vary a lot depending on its configurations and/or operation modes, the hierarchical control of an inverter-interfaced microgrid proposed in Guerrero et al. (2011) has been widely recognized as a general approach towards standardization. The hierarchy typically consists of three layers, namely, the primary control layer, the secondary control layer, and the tertiary control layer, among which the latter two are conventionally based on a microgrid central controller (MGCC). Therefore, any failure of connection between the MGCC and every single unit could adversely result in instability of the entire microgrid. Furthermore, massive data to be processed, along with centralized calculations of the optimal setpoints to the various microgrid units, imposes a considerable computational burden on the MGCC. This implies that the control approaches currently in use are not scalable and are highly prone to single-point-of-failure. Distributed control schemes can address these issues since they allocate the computational tasks to every participant and, by permitting information exchange only with neighbors, they are more reliable, not sensitive to single-point-of-failure and economic-friendly. Furthermore, distributed control schemes can also address privacy-related concerns since they do not require sensitive data to be sent to the microgrid operator.

To this end, the idea of breaking the hierarchy was proposed initially in Dörfler et al. (2016). The authors in Li et al. (2014) further investigated the inherent common features between frequency control and economic dispatch in a power grid, fully demonstrating the potential of gradient algorithms. More recently, the application of the distributed gradient algorithm was extended to the field

[1] This work was partially supported by the EC H2020 'Border management of variable renewable energies and storage units enabling a translational Wholesale market (CROSSBOW)' project.

of microgrid, as reported in Zhao and Ding (2017), managing frequency deviations caused by load fluctuations by considering a proportional relationship between frequency deviation and active power mismatch. However, it is now of great benefit to using a more realistic model, where hierarchical architecture preserved. Moreover, very little was found in the literature on the benefits of demand response (DR) mechanisms for frequency restoration in spite of progress in coordinating multiple inverter-based DG units had been achieved.

The ideas illustrated above are further developed to facilitate the design of the optimal frequency restoration strategy, to a droop-controlled inverter-interfaced microgrid through distributed energy management. The objective function of the energy management problem is formulated to minimize the overall cost of all participants in the microgrid, including DG units and demand-side customers. The Multi-Agent System (MAS) is developed by assigning each bus a bus agent (BA) that only has access to information of its neighbors through a communication network. Besides, the network-preserving model is adopted in this paper to describe the couplings among neighboring buses and inverters. Furthermore, as few modifications as possible are made to the popularized hierarchical architecture when designing the new strategy, i.e., with primary control, secondary control, and tertiary control elements retained so that the distributed algorithm can be implemented without additional investment.

The rest of the paper is organized as follows. Section II introduces the dynamic model of the entire microgrid. In Section III, the detailed distributed gradient algorithm is presented from the perspective of energy management, and a sufficient condition for frequency restoration is given. In Section IV, the effectiveness of the distributed algorithm is validated via simulation studies on a 6-bus test system. Section V concludes the paper.

2. MODELING OF A MICROGRID

2.1 DG Model

Considering that other loops in the primary controller (i.e., voltage control loop, current control loop, etc.) are much faster than the droop control loop, we model the inverter as an ideal voltage source, where all internal control loops except the droop control loop can be ignored.

The universal principle behind the droop control could be explained as increasing the frequency when the active power is low to mimic the operation of a synchronous generator. In this paper, the well-known $P-\omega$ control is employed to regulate the inverter voltage phase angle δ_i by comparing the local measurement of active power P_i^m with the desired value P_i^d. According to Yu et al. (2011), we adopt the typical proportional controller, and the inverter at bus i is modeled as follows:

$$\dot{\delta}_i = \omega_i^g, \tag{1a}$$

$$\omega_i^g = \omega^d - k_{P_i}(P_i^m - P_i^d), \tag{1b}$$

where ω_i^g and ω^d are respectively the inverter frequency deviation and its desired value, while the active power P_i is measured and processed through a first-order low-pass filter, giving that $\tau_{P_i}\dot{P}_i^m = -P_i^m + P_i$. Here, τ_{P_i} denotes

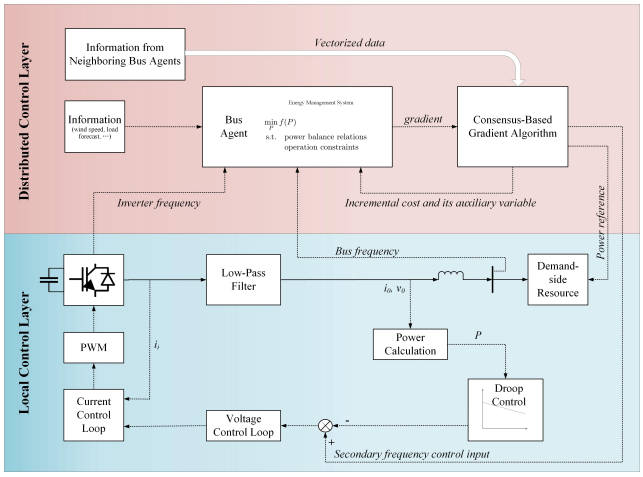

Fig. 1. Block diagram of proposed control architecture.

the time constant of the first-order low-pass filter. Then, we have the simplified closed-loop dynamics of the inverter voltage frequency, which is given by

$$\tau_{P_i}\dot{\omega}_i^g + \omega_i^g - \omega^d + k_{P_i}(P_i - P_i^d) = 0. \tag{2}$$

2.2 Network-Preserving Model

Consider a microgrid consisting of N buses, to which at most a DR unit or an inverter-interfaced DG unit is attached, and let $Y_{ij} = G_{ij} + jB_{ij}$ be the admittance of transmission line connecting bus i and j, where G_{ij} and B_{ij} represent the conductance and susceptance, respectively. In general, it is reasonable to assume all transmission line impedances have an identical R/X ratio, denoted by ρ, and, accordingly, we can deduce that $G_{ij} = -\rho B_{ij}$. Under this circumstance, the encountered power losses are non-negligible and therefore dealt with in Section 3.3.

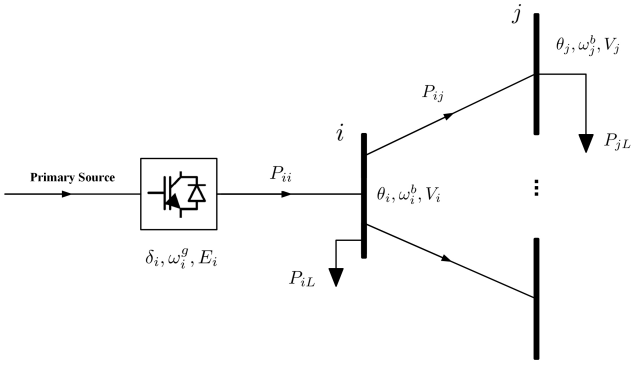

Fig. 2. Summary of notations in the network-preserving model

By assuming no shunt conductance, the active power flow from bus i to j can be derived as

$$P_{ij} = G_{ij}V_i^2 - V_iV_j(G_{ij}\cos(\theta_i - \theta_j) + B_{ij}\sin(\theta_i - \theta_j)), \tag{3}$$

where $V_i\angle\theta_i$ denotes the bus voltage. See Kundur et al. (1994) for more elaboration.

Apart from most of the relevant works, in this paper, the inverter and load bus are treated as two entities, with disparate dynamic models but coupled by power flow P_{ii}. Similar to Guo et al. (2015); Schiffer et al. (2014),

a common assumption of purely inductive output line impedance needs to be introduced, which can be fulfilled by properly tuning virtual output impedances to dominate over any resistive effects. According to the difference in voltage phase angles between inverter and bus, we can determine the active power output of the DG at bus i, which is given by

$$P_{ii} = \frac{E_i V_i}{X_i} \sin(\delta_i - \theta_i), \tag{4}$$

where the inverter voltage and output impedance is denoted by $E_i \angle \delta_i$ and X_i, respectively. The aforementioned assumption subsequently allows the parallel operation of active and reactive power loops. Therefore, we focus only on the active power control in this paper.

2.3 Dynamics of Voltage Phase Angles

In literature, droop methods have been widely established for inverter-interfaced microgrids in the presence of network-reduced models. However, when extended to network-preserving models, the droop methods need to be reformulated in order to facilitate the different scenarios. From the point of view of local power mismatch, it can be easily obtained that $P_i - P_i^d = P_{ii} - P_{iG}^d$, where P_{iG}^d the nominal output power of the DG unit at bus i. Denote the set of all buses as $\mathcal{S}$, the buses equipped with DG units as $\mathcal{S}_G$, the else with DR units can be represented by $\mathcal{S}_D = \mathcal{S} \backslash \mathcal{S}_G$. Without losing generality, we set ω^d to 0, and then, integration of (2)-(4) yields

$$\dot{\theta}_i = \omega_i^b, \quad i \in \mathcal{S} \tag{5a}$$

$$0 = -D_i \omega_i^b + P_{ii} - \sum_{j \in \mathcal{N}_i} P_{ij} - P_{iL}, \quad i \in \mathcal{S}_G \tag{5b}$$

$$0 = -D_i \omega_i^b - \sum_{j \in \mathcal{N}_i} P_{ij} - P_{iL} - P_{iD}, \quad i \in \mathcal{S}_D \tag{5c}$$

$$\dot{\delta}_i = \omega_i^g, \quad i \in \mathcal{S}_G \tag{5d}$$

$$0 = \tau_{P_i} \dot{\omega}_i^g + \omega_i^g + k_{P_i}(P_{ii} - P_{iG}^d) + u_i, \quad i \in \mathcal{S}_G, \tag{5e}$$

where ω_i^b is the frequency deviation at bus i, D_i is the damping factor of bus i, and u_i^ω is the secondary frequency control input used to compensate the frequency deviations and voltage offsets induced by primary control. In the above equation, (5a), (5b), and (5c) are models of bus voltage phase angle, whilst (5d) and (5e) are models of inverter voltage phase angle.

3. OPTIMAL FREQUENCY RESTORATION

In this section, we first give the control objective in terms of how the energy management problem relates to the optimal frequency restoration. Then we provide an approach to integrate the primary and secondary control features into the formulation of the energy management problem at the tertiary control layer. Finally, We propose our distributed consensus-based algorithm and give its convergence analysis.

3.1 Control Objective

The control objective is to restore system frequency while ensuring active power is shared cost-effectively. It has been suggested in the introduction that energy management may be an effective alternative to the classical frequency restoration. To this end, we firstly conclude the condition for the synchronization of a lossless microgrid, which is given by

$$\omega^{syn} = \omega^n + \frac{\sum\limits_{i \in \mathcal{S}_G} P_{iG} - \sum\limits_{i \in \mathcal{S}} P_{iL} - \sum\limits_{i \in \mathcal{S}_D} P_{iD}}{\sum\limits_{i \in \mathcal{S}_G} (1/k_{P_i}) + \sum\limits_{i \in \mathcal{S}} D_i}, \tag{6}$$

where P_{iG} is artificially created as the steady-state active power output of the DG unit at bus i, i.e., $P_{iG} \triangleq (P_{ii})_s$. As it can be clearly seen from (5e), $P_{iG} = P_{iG}^d - (u_i^\omega + \omega^{syn} - \omega^n)/k_{P_i}$, confirming that as long as the total distributed generation $\sum_{i \in \mathcal{S}_G} P_{iG}$ is different from the total power consumption $\sum_{i \in \mathcal{S}} P_{iL} + \sum_{i \in \mathcal{S}_D} P_{iD}$, the synchronized frequency ω^{syn} will deviate from the natural frequency ω^n.

Summarizing, these findings provide an appropriate starting point for combining energy management with frequency restoration, that is, taking the power balance as an equality constraint in the energy management problem. Subsequently, the frequency restoration can be realized with appropriate agent preference setups.

3.2 Problem Formulation

1) Demand-side resource. According to Rahbari-Asr et al. (2014), demand-side resource refers to customers who actively participate in the demand response program and provide auxiliary services. Typically, the DR welfare W_i quantifies the level of satisfaction determined by its energy consumption, which can be described by

$$W_i(P_{iD}) \triangleq \begin{cases} \alpha_i P_{iD}^2 - \beta_i P_{iD}, & P_{iD}^{\min} \le P_{iD} \le \beta_i / 2\alpha_i \\ -\beta_i^2 / 4\alpha_i, & \beta_i / 2\alpha_i \le P_{iD} \le P_{iD}^{\max} \end{cases}, \tag{7}$$

where $P_{iD}^{\min}$, $P_{iD}^{\max}$, α_i, and β_i are parameters specified by agent preference and customers' behavior. It should be pointed out that the cost function is convex without switching dynamics and will not lead to the loss of the convexity structure of the problem.

2) DG unit. The power generation cost of the DG unit at bus i depends to some extent on how the output power deviates from the rated power, which can be constructed as

$$C_i(P_{iG}) \triangleq a_i {P_{iG}}^2 + b_i P_{iG} + c_i, \tag{8}$$

where $a_i = \epsilon_i / 2P_{iG}^d$, $b_i = -\epsilon_i$, and $c_i = \epsilon_i P_{iG}^d / 2$, accordingly. ϵ_i is introduced as a coefficient to indicate the trade-off between generated power and the corresponding cost, which can be selected according to the nominal output power, installation cost, and maintenance cost. Interested readers please refer to Domínguez-García et al. (2012) for further details. Afterwards, we may conclude that the lowest generation cost is achieved when the deviation of P_{iG} from P_{iG}^d is minimized. This reveals that the optimal frequency control can be achieved by properly adjusting the secondary frequency control input u_i^ω. Certainly, there are bounds on u_i^ω, which are consequently reflected as $P_{iG}^{\min}$ and $P_{iG}^{\max}$.

Recall (5e) and (6), the frequency aspects are implicitly addressed in P_{iG}, and thence, the energy management problem located at the tertiary control layer, establishing

the optimal operation of the microgrid to minimize operational cost, can be formulated by minimizing the operation cost with the generation and DR constraints as follows:

$$\min_{P_{iD},P_{iG}} \sum_{i\in\mathcal{S}_G} C_i(P_{iG}) - \sum_{i\in\mathcal{S}_D} W_i(P_{iD}), \tag{9a}$$

$$\text{s.t.} \quad \sum_{i\in\mathcal{S}_G} P_{iG} = \sum_{i\in\mathcal{S}} P_{iL} + \sum_{i\in\mathcal{S}_D} P_{iD}, \tag{9b}$$

$$P_{iD}^{\min} \le P_{iD} \le P_{iD}^{\max}, \quad i \in \mathcal{S}_D, \tag{9c}$$

$$P_{iG}^{\min} \le P_{iG} \le P_{iG}^{\max}, \quad i \in \mathcal{S}_G. \tag{9d}$$

3.3 Distributed Consensus Algorithm

Let $u_i = P_{iG}$ and $\kappa_i = 1$ for $i \in \mathcal{S}_G$, and let $u_i = P_{iD}$ and $\kappa_i = -1$ for $i \in \mathcal{S}_D$, (9) can be reformulated in the standard form as

$$\min_{u_i} \sum_{i=1}^{N} f_i(u_i), \tag{10a}$$

$$\text{s.t.} \quad \sum_{i=1}^{N} \kappa_i u_i = \sum_{i=1}^{N} \xi_i d_i, \tag{10b}$$

$$u_i^{\min} \le u_i \le u_i^{\max}, \quad i = 0, 1, 2, ..., N, \tag{10c}$$

where $d_i = P_{iL}$, and $\xi_i > 1$ is a coefficient to compensate power losses and is selected by a loss allocation procedure by solving an Optimal Power Flow (OPF) problem, which is in a much slower time-scale and out of the scope of this paper. It is easily perceived that this is a convex optimization problem with affine constraints. Letting $L(u_i, \lambda_i)$ be the Lagrangian function, we have

$$L(u_i, \lambda_i) = \sum_{i=1}^{N} f_i(u_i) + \sum_{i=1}^{N} \lambda_i(\kappa_i u_i - \xi_i d_i), \tag{11}$$

where λ_i is the Lagrangian multiplier. One thing worth noting is that the inequality constraints are local, and their presence or absence does not even affect the convergence. Hence, the inequality constraints are needless to be included in the Lagrangian function, and they are handled as the boundaries of the problem domain.

Following the Karush-Kuhn-Tucker (KKT) conditions reported in Boyd and Vandenberghe (2004), a point $u^* = [u_1^*, ..., u_n^*]^{\mathrm{T}}$ is the optimal solution of (10) iff there exists a point λ^* such that

$$\frac{\partial L}{\partial u_i} = \nabla f(u_i) + \kappa_i \lambda^* = 0, \tag{12a}$$

$$\frac{\partial L}{\partial \lambda^*} = \sum_{i=1}^{N} (\kappa_i u_i - \xi_i d_i) = 0. \tag{12b}$$

It implies the Lagrangian multiplier λ_i, which has been associated with the economic meaning of incremental cost, should converge to the same value. Inspired by Zhao and Ding (2018), we propose the novel consensus-based gradient algorithm written in a compact form as follows:

$$\dot{u} = -\nabla f(u) - \kappa\lambda - \gamma_1\omega^g - \gamma_2\omega^b, \tag{13a}$$

$$\dot{\lambda} = -\eta_1\mathcal{L}\lambda - \eta_2\mathcal{L}z + \eta_3(\kappa u - \xi d), \tag{13b}$$

$$\dot{z} = \mathcal{L}\lambda, \tag{13c}$$

where $\mathcal{L}$ represents the Laplacian matrix that describes the communication topology among agents, $u = [u_1, ..., u_n]^{\mathrm{T}}$, $\nabla f(u) = \partial \sum_{i=1}^{N} f_i(u_i)/\partial u_i$, $\lambda = [\lambda_1, ..., \lambda_n]^{\mathrm{T}}$, $z = [z_1, ..., z_n]^{\mathrm{T}}$, $d = [d_1, ..., d_n]^{\mathrm{T}}$, $\kappa = \mathrm{diag}(\kappa_1, ..., \kappa_n)$, and $\xi = \mathrm{diag}(\xi_1, ..., \xi_n)$, respectively. γ_1 and γ_2 are both positive semidefinite diagonal matrices, whilst η_1, η_2, η_3 are all positive definite constants. It is noted that λ_i is estimated with only the adjacent information and, more specifically, z_i is an auxiliary variable employed to ensure the consistency of λ_i. Two terms, i.e., $\gamma_1\omega^g$ and $\gamma_2\omega^b$, are employed to steer control performance towards frequency restoration objectives by eliminating steady-state deviations and achieving faster convergence speed.

3.4 Convergence Analysis

To conduct convergence analysis for the proposed algorithm, we assume the microgrid is lossless such that (3) can be replaced by $P_{ij} = V_iV_j|B_{ij}|\sin(\theta_i - \theta_j)$, where $|B_{ij}|$ is the magnitude of B_{ij}. Analogous to Wang et al. (2019), we explicitly construct a Lyapunov candidate function, composed of three parts: the potential energy part, the frequency part, and the quadratic part, which is given by

$$\begin{aligned} V = &\underbrace{W_p(\eta) - (\eta - \eta^*)\nabla_\eta W_p(\eta) - W_p^*(\eta^*)}_{V_p} \\ &+ \underbrace{\sum\nolimits_{i\in\mathcal{S}_G} \frac{\tau_{P_i}}{2k_{P_i}}\tilde{\omega}_i^{g2}}_{V_\omega} + k\underbrace{(\tilde{u}^{\mathrm{T}}\tilde{u} + \tilde{\lambda}^{\mathrm{T}}\tilde{\lambda} + \tilde{z}^{\mathrm{T}}\tilde{z})}_{V_k}, \end{aligned} \tag{14}$$

where $\eta \triangleq [\delta, \theta]^{\mathrm{T}}$, $\tilde{\omega}_i^g = \omega_i^g - \omega_i^{g*}$, $\tilde{\omega}_i^b = \omega_i^b - \omega_i^{b*}$, $\tilde{u}_i = u_i - u_i^*$, $\tilde{\lambda} = \kappa M^{\mathrm{T}}(\lambda - \lambda^*)$, and $\tilde{z} = M^{\mathrm{T}}(z - z^*)$. M is an orthonormal matrix such that $M^{-1} = M^{\mathrm{T}}$. Notably, the concept of Bregman is introduced, see De Persis and Monshizadeh (2018), to construct the potential energy part of the Lyapunov function

$$\begin{aligned} W_p = &-1/2\sum\nolimits_{i\in\mathcal{S}}\sum\nolimits_{j\in\mathcal{N}_i} V_iV_jB_{ij}\cos(\theta_i - \theta_j) \\ &- \sum\nolimits_{i\in\mathcal{S}_G} E_iV_i\cos(\delta_i - \theta_i)/X_i. \end{aligned} \tag{15}$$

Taking the derivative of V_p, we have

$$\dot{V}_p = \sum\nolimits_{i=1}^{N}\sum\nolimits_{j\in\mathcal{N}_i} \tilde{P}_{ij}(\omega_i^b - \omega_j^b) + \sum\nolimits_{i\in\mathcal{S}_G} \tilde{P}_{ii}(\omega_i^g - \omega_j^b). \tag{16}$$

It is indicated by (5b) and (5c) that

$$\begin{aligned} \dot{V}_\omega = &-\dot{V}_p - \sum\nolimits_{i\in\mathcal{S}_G} \frac{1}{k_{P_i}}\tilde{\omega}_i^{g2} - \sum\nolimits_{i\in\mathcal{S}} D_i\tilde{\omega}_i^{b2} \\ &+ \sum\nolimits_{i\in\mathcal{S}_G} \kappa_i\tilde{\omega}_i^g\tilde{P}_{iG} + \sum\nolimits_{i\in\mathcal{S}_D} \kappa_i\tilde{\omega}_i^b\tilde{P}_{iD}. \end{aligned} \tag{17}$$

After that, taking the derivative of V_k, it claims

$$\begin{aligned} \dot{V}_k = &-\eta_3\underbrace{\tilde{u}^{\mathrm{T}}(\nabla f(u) - \nabla f(u^*))}_{\phi_1} - \eta_1\underbrace{\tilde{\lambda}^{\mathrm{T}}M^{\mathrm{T}}\mathcal{L}M\tilde{\lambda}}_{\phi_2} \\ &- \gamma_1\tilde{u}^{\mathrm{T}}\tilde{\omega}^g - \gamma_2\tilde{u}^{\mathrm{T}}\tilde{\omega}^b, \end{aligned} \tag{18}$$

where $\phi_1 \ge 0$ and $\phi_2 \ge 0$ can be guaranteed by invoking the convexity of the cost function and the positive semidefinition of $\mathcal{L}$, respectively. Along with (16) and (17), it leads to

$$\dot{V} \le \sum_{i\in\mathcal{S}_G} \kappa_i\tilde{\omega}_i^g\tilde{P}_{iG} + \sum_{i\in\mathcal{S}_D} \kappa_i\tilde{\omega}_i^b\tilde{P}_{iD} - k(\gamma_1\tilde{u}^{\mathrm{T}}\tilde{\omega}^g - \gamma_2\tilde{u}^{\mathrm{T}}\tilde{\omega}^b). \tag{19}$$

Consequently, one sufficient condition for $\dot{V} \le 0$ is $k[\gamma_1]_{ii} = \kappa_i$ for $i \in \mathcal{S}_G$ and $k[\gamma_2]_{ii} = \kappa_i$ for $i \in \mathcal{S}_D$.

According to the Lyapunov Stability theory and LaSalle's invariance principle reported in Khalil (2002), the system converges to its equilibrium point if and only if $\dot{V} \leq 0$, which means ω_i^g and u_i will converge to 0 and u_i^*, respectively; hence, the optimal frequency restoration can be realized.

4. SIMULATION STUDY

A 6-bus microgrid shown in Fig. 3 is adopted as the test system in order to verify the effectiveness of the proposed control algorithm, and the simulation is conducted in MATLAB/Simulink environment. The microgrid is composed of three inverter-based DG units, three DR units, and six respective loads. Additionally, transmission lines are modeled as impedances with ρ equal to 0.4. The microgrid is considered to operate in the islanded-mode with a nominal voltage of 310 V and a nominal frequency of 50 Hz. To highlight the wide applicability of the proposed algorithm, we set the physical graph and the communication graph as two different graphs, as shown in Fig. 3. The parameters of the test system are modified from Guo et al. (2015), e.g., the rated active power for DG1, DG2, and DG3 are respectively 50 kW, 100 kW, and 150 kW.

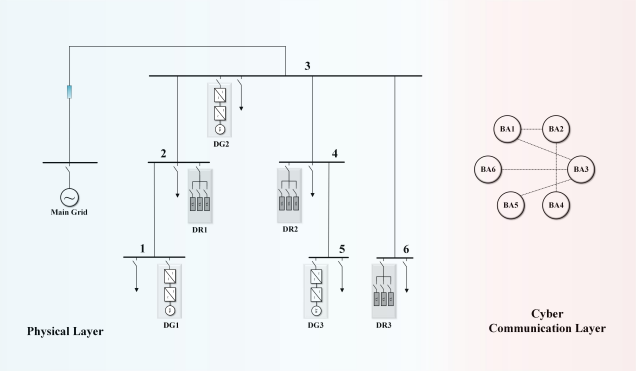

Fig. 3. Single-line diagram and communication topology of the test microgrid

This section is organized into two case studies, starting with generation intermittency and then generation perturbation. In both scenarios, we assume regular operation, i.e., all grid-forming units work at their rated power, at the initial time $t = 0$ s, followed by a disturbance that occurs at $t = 20$ s. Although $Q - V$ control is not being discussed in this paper, we introduce Gaussian noise into each inverter and bus to emulate the variations in voltage amplitudes.

4.1 Generation Intermittency

Here we proceed with a scenario of generation intermittency, namely, the maximum output power of DG1 drops from 55 kW to 25 kW, restricted by the primary source input (e.g., illumination intensity and wind speed). As illustrated in Fig. 4, the frequency is well restored to the nominal value within a settling time of about 1.7 s, while the incremental costs undergo a significant oscillation and take another 5 s to converge to a relatively higher value but do not affect the frequency stability at all. It can also be observed that, after the disturbance occurs, the secondary frequency control inputs of DG2 and DG3 tend to be identical, demonstrating proportional active power-sharing is re-achieved, though some adjustments have been made according to the needs in compensating power losses.

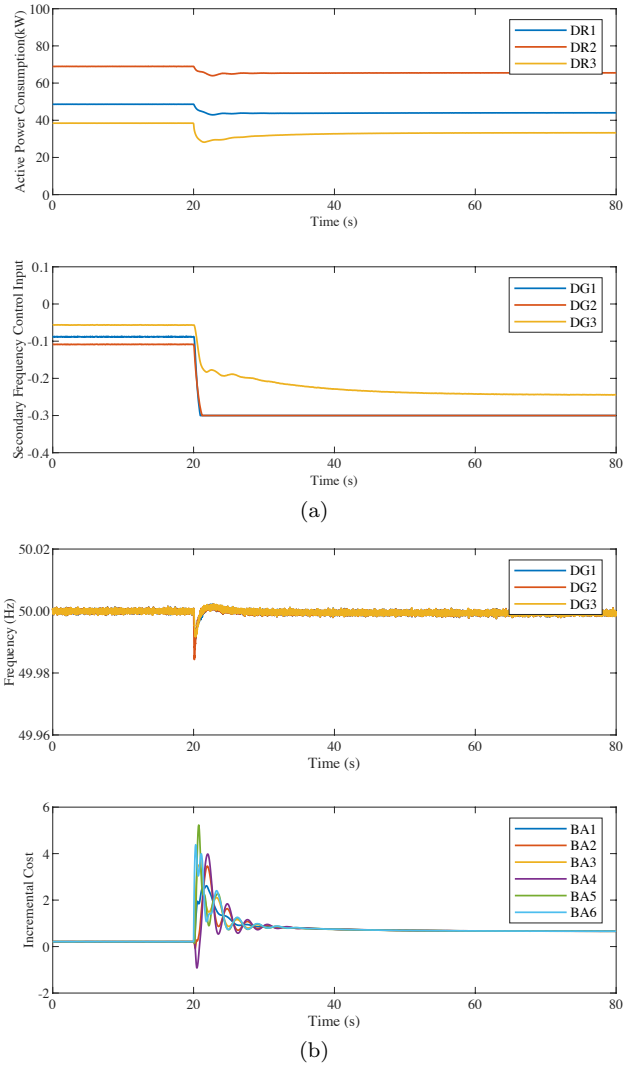

Fig. 4. Evolution of (a) inverter frequency and incremental cost, (b) DR unit power consumption and secondary frequency control input under generation intermittency.

4.2 Load Perturbation

Considering the network-preserving model adopted, we can speculate that the influence caused by a disturbance on the inverter side may be different from that on the bus side, for which simulation study is carried out. We specify an increase in load demand at bus 6 from 40 kW to 70 kW at $t = 20$ s. As shown in Fig. 5, the frequency deviation, which is less remarkable compared with Fig. 4(a), is quickly eliminated as demand-side customers are encouraged to lower consumption, and secondary frequency control inputs are tuned to increase outputs, to balance power mismatch. Besides, the influence of power loss is avoided, that is, no steady-state deviation is found. These coincide with the conclusion for the previous case study. Thus, the proposed algorithm is also sufficiently compelling under load perturbation. Given the performance after variations in voltage

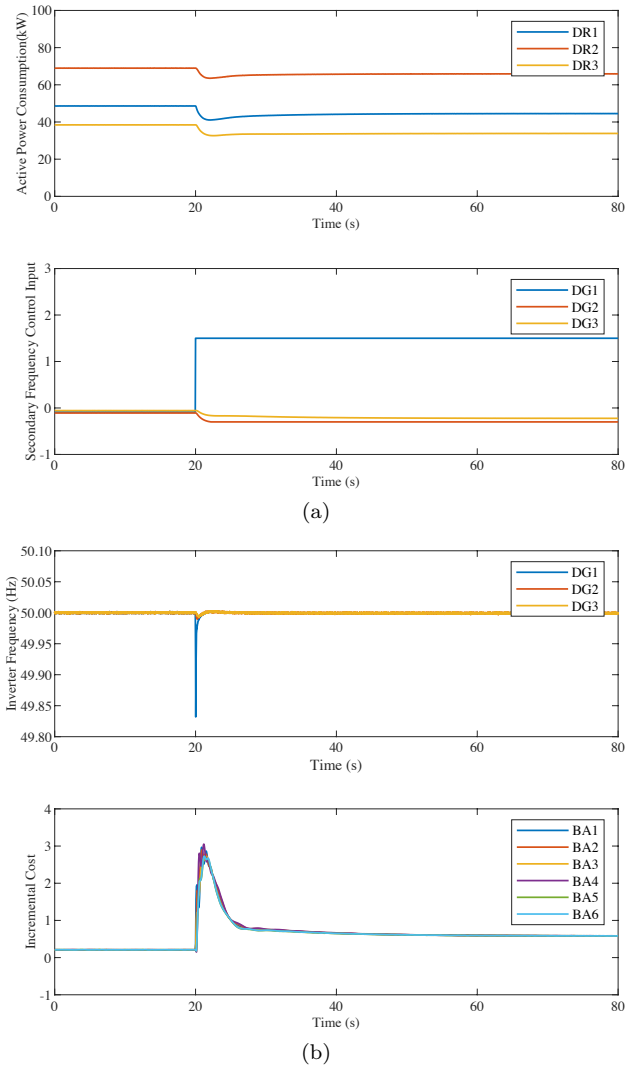

Fig. 5. Evolution of (a) inverter frequency and incremental cost, (b) DR unit power consumption and secondary frequency control input under load perturbation.

amplitudes are already included, we can convince that the proposed strategy can still achieve the expected control effect under the parallel operation of active/reactive power controls.

5. CONCLUSION

In this paper, we introduce a consensus-based gradient algorithm for frequency restoration based on distributed energy management in an islanded inverter-interfaced microgrid. Both the DR units and the DG units are taken into account as dispatchable resources, and the network-preserving model is deployed to prevent loss of network topology and transient characteristics as well. Finally, the control performance of the proposed distributed algorithm is assessed under different disturbances, which demonstrate that our algorithm can well coordinate various participants, promptly eliminate frequency deviations, and achieve the cost-effective operation of a generic microgrid.

REFERENCES

Boyd, S. and Vandenberghe, L. (2004). *Convex optimization*. Cambridge university press.

De Persis, C. and Monshizadeh, N. (2018). Bregman storage functions for microgrid control. *IEEE Transactions on Automatic Control*, 63(1), 53–68.

Dimeas, A.L. and Hatziargyriou, N.D. (2005). Operation of a multiagent system for microgrid control. *IEEE Transactions on Power Systems*, 20(3), 1447–1455.

Domínguez-García, A.D., Cady, S.T., and Hadjicostis, C.N. (2012). Decentralized optimal dispatch of distributed energy resources. In *2012 IEEE 51st IEEE Conference on Decision and Control (CDC)*, 3688–3693.

Dörfler, F., Simpson-Porco, J.W., and Bullo, F. (2016). Breaking the hierarchy: Distributed control and economic optimality in microgrids. *IEEE Transactions on Control of Network Systems*, 3(3), 241–253.

Guerrero, J.M., Vasquez, J.C., Matas, J., de Vicuna, L.G., and Castilla, M. (2011). Hierarchical control of droop-controlled ac and dc microgrids—a general approach toward standardization. *IEEE Transactions on Industrial Electronics*, 58(1), 158–172.

Guo, F., Wen, C., Mao, J., and Song, Y. (2015). Distributed secondary voltage and frequency restoration control of droop-controlled inverter-based microgrids. *IEEE Transactions on Industrial Electronics*, 62(7), 4355–4364.

Katiraei, F. and Iravani, M.R. (2006). Power management strategies for a microgrid with multiple distributed generation units. *IEEE Transactions on Power Systems*, 21(4), 1821–1831.

Khalil, H. (2002). Nonlinear systems. *Upper Saddle River*.

Kundur, P., Balu, N., and Lauby, M. (1994). *Power system stability and control*, volume 7. McGraw-hill New York.

Lasseter, R.H. and Paigi, P. (2004). Microgrid: a conceptual solution. In *2004 IEEE 35th Annual Power Electronics Specialists Conference (IEEE Cat. No.04CH37551)*, volume 6, 4285–4290 Vol.6.

Li, N., Chen, L., Zhao, C., and Low, S.H. (2014). Connecting automatic generation control and economic dispatch from an optimization view. 735–740.

Rahbari-Asr, N., Ojha, U., Zhang, Z., and Chow, M. (2014). Incremental welfare consensus algorithm for cooperative distributed generation/demand response in smart grid. *IEEE Transactions on Smart Grid*, 5(6), 2836–2845.

Schiffer, J., Ortega, R., Astolfi, A., Raisch, J., and Sezi, T. (2014). Conditions for stability of droop-controlled inverter-based microgrids. *Automatica*, 50(10), 2457–2469.

Wang, Z., Liu, F., Pang, J.Z.F., Low, S.H., and Mei, S. (2019). Distributed optimal frequency control considering a nonlinear network-preserving model. *IEEE Transactions on Power Systems*, 34(1), 76–86.

Yu, X., Cecati, C., Dillon, T., and Simões, M.G. (2011). The new frontier of smart grids. *IEEE Industrial Electronics Magazine*, 5(3), 49–63.

Zhao, T. and Ding, Z. (2017). Optimal energy management of microgrid via distributed primal-dual dynamics for fast frequency recovery. In *2017 IEEE Power Energy Society General Meeting*, 1–5.

Zhao, T. and Ding, Z. (2018). Cooperative optimal control of battery energy storage system under wind uncertainties in a microgrid. *IEEE Transactions on Power Systems*, 33(2), 2292–2300.